

# Effect of Ethylene Maleic Anhydride on the Particulate Processes during Hydrogen Reduction of Nickel Ammine Sulphate Solutions

R.A. Iloy and F. Ntuli\*

University of Johannesburg, Johannesburg, South Africa

\*Corresponding author: [fntuli@uj.ac.za](mailto:fntuli@uj.ac.za)

The use of additives in the precipitation of nickel with hydrogen is known to influence the particulate processes and, by extension, powder properties such as morphology, microstructure and particle size distribution. Controlling these properties is crucial for some downstream processes. The present study assesses the effect of ethylene maleic anhydride on the particulate processes taking place during the reduction of nickel ammine sulphate solutions by hydrogen gas. Reactions were carried out in an autoclave operated at 28 bar and 180°C under stirring conditions of 850 rpm. Particulate processes were studied by analysing the particle size distribution and the corresponding normalized moments. These were further validated by scanning electron microscopy and nitrogen physisorption analyses. The powder phase identification and purity were determined by means of X-ray diffraction and X-ray fluorescence, respectively. Ethylene maleic anhydride acted as a growth inhibitor and an anti-agglomerating agent, thus acting as a reduction catalyst by maintaining the available surface area for reduction. The system was dominated by agglomeration at low concentration (2–5 mg/L) of ethylene maleic anhydride while breakage became the dominant particulate process at higher concentration (7–10 mg/L), as validated by scanning electron micrographs.

## INTRODUCTION

Hydrogen reduction is the most efficient and widely used method to precipitate metal powders from solutions (Meddings and Mackiw, 1965; Agrawal et al., 2006). Approximately 240 000 tons of nickel alone is produced this way per year worldwide. Commercial operations using this technology include, among others, Impala Platinum (South Africa), Sherritt (Canada) and Murrin Murrin (Australia) (Crundwell et al., 2011). Hydrogen reduction is a process whereby an ammoniacal aqueous metal salt solution is subjected to hydrogen at elevated pressure and temperature in mechanically agitated autoclaves. Under these conditions, the dissolved metal ions undergo reduction and precipitate as metallic powders. The possibility of precipitating metals from solutions using gases as reducing agents was first established by Beketov in the 1860s (Agrawal et al., 2006). The earliest interest was in the reduction of copper sulphate solutions using sulphur dioxide and carbon monoxide as reducing agents. The use of hydrogen as a reducing agent was investigated during the period 1909– 1931 in the precipitation of metals from their aqueous and organic solutions. In these investigations, reactions were done at elevated hydrogen pressure and temperature in sealed and non-agitated tubes. As a result, products were contaminated with stable oxides and basic salts (Evans, 1968). The commercialization of the hydrogen reduction process was made possible by Chemical Construction Corporation in the 1950s after extensive research and developmental work (Habashi, 1999, Osseo-Asare, 2013).

Since the commercialization of gaseous reduction technology, additives or addition agents have been identified as playing a major role in the operation of the process. In fact, in this process the precipitated metals have the tendency to agglomerate and plate out on the impeller of the agitator and the walls of the reaction vessel. Addition agents assist in lessening the surface activity of the reduced metal particles and therefore inhibit plating and agglomeration. Furthermore, they accelerate the reaction, making it possible to achieve reduction at shorter periods of time. They also help in controlling the physical characteristics of the obtained powder, such as morphology, size and density, which constitute important parameters for downstream processes (Chou et al., 1976; Saarinen et al., 1998; Agrawal et al., 2006; Luidold and Antrekowitsch, 2007; Naboychenko et al., 2009). As an example, in fuel cell technologies, the porosity of materials used to construct the electrodes is a critical parameter, amongst others. These elements together contribute to making the gaseous reduction technology commercially viable. However, commercial additives are quite expensive and, in most cases, their function and mechanism of action are not well understood, with most of them being employed on a trial-and-error basis (Bodoza et al., 2013). Because additives are normally one of the major operational costs, developing an understanding of their mechanism of action will enable their optimum use in industry.

The aim of this study was to investigate the function and mechanism of action of ethylene maleic anhydride (EMA) as an additive in high-pressure hydrogen reduction of ammoniacal nickel sulphate solutions. This additive has been reported (Kunda and Campbell, 1972) to alter the metal powder physical properties at concentrations as low as 5 mg/L. The choice of this additive was prompted by the contradictory data found in published literature. While ethylene maleic anhydride has been reported (Kunda et al., 1965) in one study to have no influence on the reduction rate and promote agglomeration, a different set of experiments (Bodoza et al., 2013) suggested the opposite. It was found that the reduction rate could be increased by a factor of three, depending on the modifier dosage. Moreover, the modifier prohibited agglomeration with increasing dosage up to 7 mg/L. This paper intends to address these contradictions by particle size distribution modelling, along with scanning electron microscopy.

## EXPERIMENTAL

### Apparatus

Experiments were conducted in a 750 mL laboratory-scale stainless steel (SS 316) autoclave with a maximum allowable working pressure of 100 bar that could be operated at temperatures up to 250°C. The autoclave height and internal diameter were 193 mm and 75 mm, respectively. Agitation was achieved by a double-pitched six-bladed turbine impellers (diameter 35 mm) with a spacing of 60 mm mounted on a shaft driven by a 0.18 kW electric motor. The lower impeller had an off-bottom clearance of 10 mm. Other internal parts of the autoclave included a serpentine cooling coil, a thermowell housing a thermocouple and a dip tube through which gases were admitted. Heating was achieved by means of an electric heating mantle (1.25 kW) around the vessel and controlled by means of a control panel with a proportional-integral-differential (PID) temperature controller. The same control panel also allowed for the motor speed to be adjusted in terms of number of revolutions per minute (rpm), which could be varied from 50 to 1450 rpm. Pressure readings were made possible by a bourdon type pressure gauge with a range of 0–100 bar.

### Reduction Procedure

The pressure reactor was first loaded with 450 mL of the nickel solution prepared as described by Ntuli and Lewis (2007), 30 g of nickel powder as seeding material and a predetermined amount of EMA. On the controller, the temperature and agitation speed were then set to 180°C and 850 rpm, respectively. To expel oxygen from the system, the reactor was successively flushed with nitrogen and hydrogen gases at 10 bar. As soon as the reactor temperature reached 175°C, hydrogen was introduced to the reaction vessel, bringing the system pressure to 28 bar. The hydrogen supply to the system was kept constant throughout reduction. At the end of reduction, agitation and heating were stopped. The reactor was allowed to cool down and depressurised before discharging its content. The nickel-depleted

reduction solution and powder thus obtained were separated by decantation. The spent solution was kept for analysis to determine the residual nickel concentration and the powder was used as seeding material for the next densification. This process was repeated for up to five densifications, at the end of which the powder was finally collected, washed and dried in an oven at 80°C. The powder so obtained was weighed and characterized. All experiments were duplicated and the average values reported where applicable.

### **Instrumental Analyses**

Atomic absorption spectrophotometry (Thermo Scientific ICE 3000 series) was used to determine nickel concentration in the prepared solution for reduction and the resulting spent solutions. Laser diffraction was used for particle size distribution analysis using a Mastersizer 2000 equipped with a wet dispersion unit (Hydro 2000G) manufactured by Malvern Instruments. This instrument is capable of measuring particle sizes from 0.02 to 2000  $\mu\text{m}$ . In a typical analysis, the sample is prepared and introduced into the dispersion unit where it is dispersed to the correct concentration before being delivered to the optical bench. The purity of the original nickel powder and that obtained after five densifications with different EMA concentrations were determined by X-ray fluorescence analysis (XRF) using a Rigaku ZSX Primus II equipped with a rhodium target at 50 kV and 40 mA. Sample preparation consisted of making the powder into pellets by means of a hydraulic press. X-ray diffraction was used to identify the crystalline phases present in the nickel powder before and after reduction at different additive levels using a Rigaku Ultima IV diffractometer equipped with a copper target. The voltage and current at which the diffractometer was operated were 40 kV and 30 mA, respectively. Spectra were acquired in the range of  $2\theta$  from 10° to 90° with a step size of 0.01° at the scanning speed of 1°/min. Scanning electron microscopy (SEM) was performed to visualize the surface morphology and the structure of particles and agglomerates in the nickel powder samples. This was carried out using a TESCAN microscope coupled with an energy-dispersive X-ray spectrometer (EDX). The information on surface area and porosity of the nickel powder was obtained by means of physisorption with nitrogen gas using Micromeritics TriStar 3000. Degassing was carried out at 90°C overnight with nitrogen gas.

## **RESULTS AND DISCUSSION**

### **Volume Distributions**

Figure 1 shows the volume-based particle size distribution of nickel powder obtained after five densifications in the absence and presence of ethylene maleic anhydride. It can be observed that the volume distributions were all bimodal. Comparing the peaks in the size range 13–182  $\mu\text{m}$  of Figure 1-A, it can be seen that the peak area after five densifications in the absence of the additive was slightly higher than that of the seeds. For the peaks at 182–955  $\mu\text{m}$ , the difference in area is hardly appreciable; however, there was a modal size shift from about 478  $\mu\text{m}$  to 363  $\mu\text{m}$ . This is an indication of particle breakage within that size region. These observations are reflected in the cumulative undersize distributions at 10%, 50% and 90% reported in Table I. A slight increase in the  $d(0.1)$  indicates size enlargement of seed particles in the smaller size fraction with subsequent densifications. This could be due to molecular growth, agglomeration or both. A sharp decrease in  $d(0.9)$  corresponds to a decrease in size in the larger size fraction. Furthermore, the slight decrease in  $d(0.5)$  suggests that larger particles were more affected than the smaller ones. This is consistent with the generally accepted view that breakage only affects larger particles or agglomerates larger than 100  $\mu\text{m}$  (Schaer et al., 2001; Ntuli and Lewis, 2009).

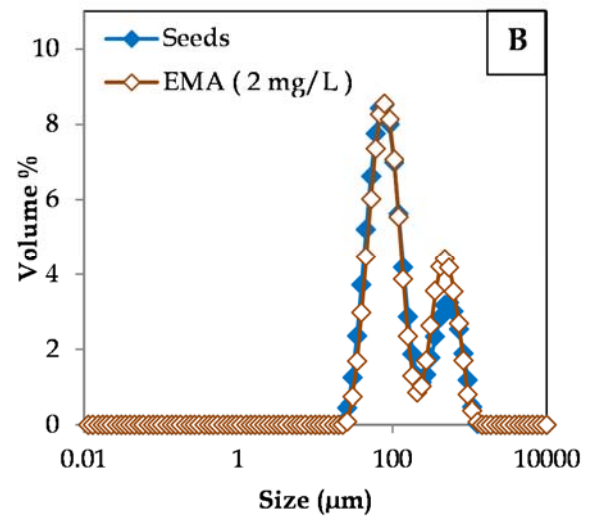
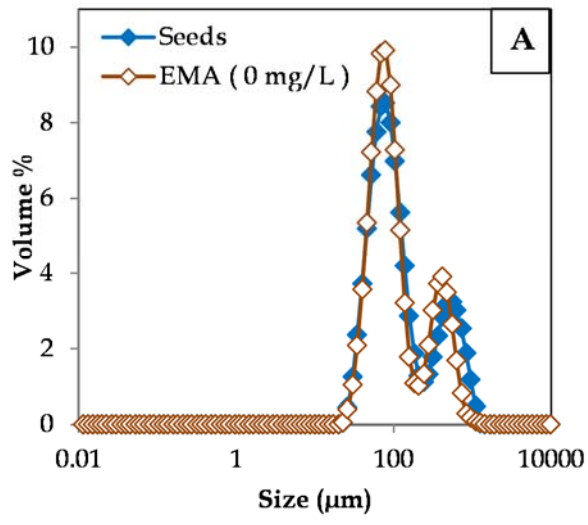
Figure 1-B shows the volume distribution of the seed and that of the nickel powder at 2 mg/L of EMA. It can be seen that major changes occurred in the larger particles region, namely the increase in the proportion of particles in the size range around 200–1100  $\mu\text{m}$ . The cumulative undersizes at 10%, 50% and 90% for different concentrations of EMA are shown in Table I. The increase in these values, together with the shape of the volume distribution, suggests that molecular growth and/or agglomeration were the dominant particulate processes.

At a concentration of 5 mg/L of EMA (Figure 1-C), it can be noticed that there was an increase in the proportion of particles in the small size region while the opposite was true for the other end of the distribution. A modal shift in the larger particles region from 478  $\mu\text{m}$  to 416  $\mu\text{m}$  for the powder obtained after five subsequent densifications indicates particle breakage, which is further confirmed by the drop in  $d(0.9)$ . The value of the  $d(0.1)$  slightly increased relative to that of the seed. This is normally attributed to molecular growth and/or agglomeration in the smaller size region. The increase in the proportion of smaller size particles could have been also a consequence of breakage by attrition of the larger particles.

The volume distribution obtained in the presence of 7 mg/L of EMA (Figure 1-D), together with the percentiles reported in Table I, show that major changes occurred in the fine and coarse fractions, while the bulk properties appeared unaffected. The decrease in the  $d(0.1)$  could be an indication of breakage. The increase in the  $d(0.9)$  suggests that either molecular growth or agglomeration took place. The extent of breakage in the coarse fraction increased as the additive concentration was raised to 10 mg/L (Figure 1-E).

*Table I. Volume distribution percentiles of the seeds and powder obtained at the fifth densification with and without EMA.*

Powder	$d(0.1)$ ( $\mu\text{m}$ )	$d(0.5)$ ( $\mu\text{m}$ )	$d(0.9)$ ( $\mu\text{m}$ )
Seed	42.40	87.49	528.44
EMA (0 mg/L)	43.13	81.48	405.32
EMA (2 mg/L)	45.79	94.17	533.55
EMA (5 mg/L)	43.36	85.70	455.13
EMA (7 mg/L)	40.69	87.38	577.01
EMA (10 mg/L)	40.02	76.75	402.12



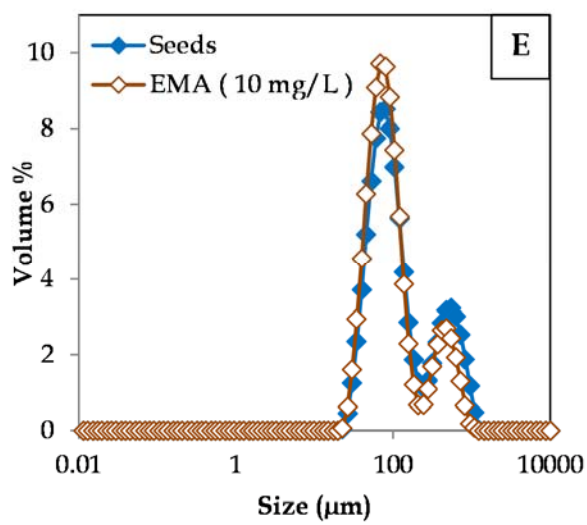
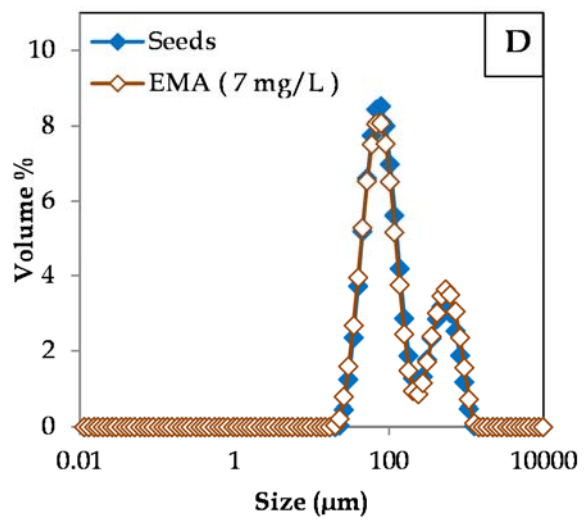
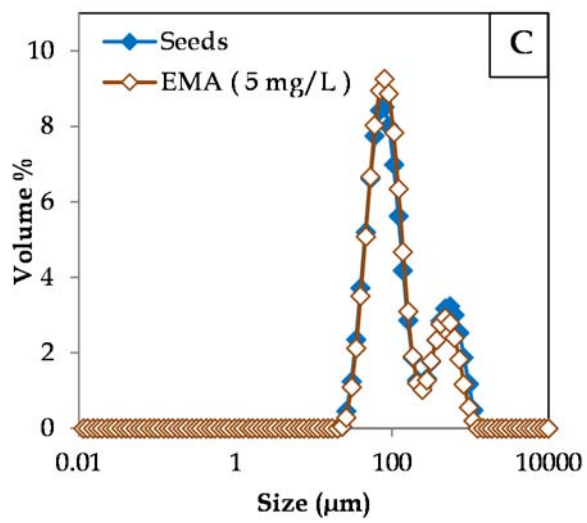


Figure 1. Volume distribution in the absence and presence of EMA.